Journal of Environmental Management 339 (2023) 117936

Contents lists available at ScienceDirect

Journal of Environmental Management

journal homepage: www.elsevier.com/locate/jenvman

Research article

Rice husk and husk biochar soil amendments store soil carbon while water management controls dissolved organic matter chemistry in well-weathered soil

Franklin Linam [a], Matt A. Limmer [a], Alina M. Ebling [b], Angelia L. Seyfferth [a,*]

[a] Department of Plant & Soil Sciences, University of Delaware, 531 S. College Avenue, Townsend Hall Rm. 152, Newark, DE, 19716, USA
[b] School of Marine Science and Policy, University of Delaware, 700 Pilottown Road, Cannon Lab Rm. 204, Lewes, DE, 19958, USA

ARTICLE INFO

Keywords:
Soil organic carbon
Dissolved organic matter
EEMs
Greenhouse gas emissions
Carbon sequestration
Rice

ABSTRACT

Rice agriculture feeds over half the world's population, and paddy soils impact the carbon cycle through soil organic carbon (SOC) preservation and production of carbon dioxide (CO_2) and methane (CH_4), which are greenhouse gases (GHG). Rice husk is a nutrient-rich, underutilized byproduct of rice milling that is sometimes pyrolyzed or combusted. It is unresolved how the incorporation of these residues affects C dynamics in paddy soil. In this study, we sought to determine how untreated (Husk), low-temperature pyrolyzed (Biochar), and combusted (CharSil) husk amendments affect SOC levels, GHG emissions, and dissolved organic matter (DOM) chemistry. We amended Ultisol paddy mesocosms and collected SOC and GHG data for three years of rice grown under alternate wetting and drying (AWD) conditions. We also performed a greenhouse pot study that included water management treatments of nonflooded, AWD, and flooded. Husk, Biochar, and CharSil amendments and flooding generally increased SOC storage and CH_4 emissions, while nonflooded conditions increased N_2O emissions and nonflooded and CharSil treatments increased CO_2 emissions. All amendments stored ~0.15 kg C m^{-2} y^{-1} more SOC than CH_4 emissions (as CO_2 equivalents), but the combustion of husk to produce CharSil resulted in the net release of CO_2 which negates any SOC storage. UV–visible absorption/fluorescence spectroscopy from the pot study suggests that nonflooded treatment decreased DOM aromaticity and molecular size. Our data show that flooding and amendment of Husk and Biochar maximized C storage in the highly weathered rice paddy soil under study despite Husk increasing CH_4 emissions. Water management affected dissolved organic matter chemistry more strongly than amendments, but this requires further investigation. Return of rice husk that is untreated or pyrolyzed at low temperature shows promise to close nutrient loops and preserve SOC in rice paddy soils.

1. Introduction

Carbon (C) is the most dynamic soil constituent and is closely intertwined with soil health and climate change. Soil organic carbon (SOC) is the dominant form of carbon in soils and has ~4 times more C than the atmosphere or biotic pool (Lal, 2004). The SOC content increases through primary productivity inputs and decreases through oxidation to carbon dioxide (CO_2), erosion, and leaching of dissolved organic carbon (DOC) (Lal, 2004). Conversion of native soils to agriculture can deplete 60–75% of SOC (Lal, 2004; Paul, 2016), but rice cultivation can preserve SOC due to high carbon inputs and flooded, suboxic conditions (Kalbitz et al., 2013), which are usually maintained for a portion of the year. This process is similar to natural wetland soils, which accumulate large amounts of SOC with long turnover times (Paul, 2016; Wu et al., 2020).

The suboxic conditions in flooded paddy soils that protect SOC also promote the production of methane (CH_4), a potent greenhouse gas. Rice agriculture is responsible for 12–26% of anthropogenic CH_4 emissions worldwide (Denman et al., 2007; Smith et al., 2007). Some studies suggest that the SOC increase in paddy soils is more than offset by CH_4 emissions (Xionghui et al., 2012). Methane is produced and consumed in soils, and most of the CH_4 emitted to the atmosphere from rice production travels through aerenchyma tissues in plants (Banker et al., 1995; Brye et al., 2013; Kludze et al., 1993; Mer et al., 2007).

* Corresponding author.
E-mail addresses: flinam@udel.edu (F. Linam), limmer@udel.edu (M.A. Limmer), aebling@udel.edu (A.M. Ebling), angelias@udel.edu (A.L. Seyfferth).

https://doi.org/10.1016/j.jenvman.2023.117936
Received 1 December 2022; Received in revised form 4 March 2023; Accepted 11 April 2023

The treatment and incorporation of crop residues into paddy soils can also affect carbon cycling. Rice straw residue incorporation can increase CH_4 emissions by a factor of 1.4–20 depending on the environmental conditions (*e.g.*, soil, temperature, and experimental design (Bossio et al., 1999; Delwiche and Cicerone, 1993; Penido et al., 2016; Xionghui et al., 2012; Ye and Horwath, 2017). Rice husk, the inedible covering of rice grain and currently an underutilized "waste" byproduct that accumulates at rice mills (Minami and Saka, 2005), does not increase CH_4 emissions as much as rice straw (Bertora et al., 2020; Gutekunst et al., 2017; Penido et al., 2016), but it is unknown what the balance between CH_4 emission and SOC storage is for untreated and pretreated rice husk amendments in paddy soil. Rice plants produce ~5 times more straw than husk, and incorporating straw can increase SOC (Bierke et al., 2008; Liu et al., 2014; Rahman et al., 2016; Xionghui et al., 2012; Zhang et al., 2012) and further protect C inputs (Chen et al., 2018), but less is known about how rice husk affects the soil C cycle. Husk has been proposed as a low-cost soil amendment that can return significant amounts of nutrients (primarily silicon as well as nitrogen, phosphorus, and potassium) to paddy soils (Gutekunst et al., 2017; Limmer et al., 2018; Linam et al., 2021; Runkle et al., 2021; Seyfferth et al., 2013, 2016, 2019; Teasley et al., 2017) and it has less arsenic than straw (Penido et al., 2016). Rice husk is sometimes pyrolyzed or combusted to biochar or ash to decrease its mass (Koyama et al., 2015). While burning rice straw residues in the field can store recalcitrant black carbon in paddy soils (Lehndorff et al., 2016), there is a lack of consensus about whether charring rice husk stores more (Haefele et al., 2011; Koyama et al., 2015), less (Koyama et al., 2016), or the same (Koyama and Hayashi, 2017) amount of SOC compared to the untreated husk.

Rice paddy soils can also emit significant quantities of the greenhouse gases CO_2 and nitrous oxide (N_2O), particularly when drained, as in nonflooded or alternate wetting and drying (AWD) water management. When O_2 enters paddy soils, N_2O is produced during the nitrification/denitrification process (Khalil et al., 2009; Verhoeven et al., 2019); this leads to a trade-off with CH_4 production (Linquist et al., 2015; Yu and Patrick, 2003). Soil incorporation of crop residues may increase N_2O emission in nonflooded conditions, though this remains unresolved (Liu et al., 2014). While CO_2 is ubiquitous in all redox/-flooding conditions, its emissions also increase with soil redox potential (Eh) (Yu and Patrick, 2003). Rice straw can increase CO_2 emissions, especially from low SOC soils (Ye and Horwath, 2017) and in nonflooded conditions (Liu et al., 2014). Data suggests that untreated (but not charred) husk may increase CO_2 as well (Koyama et al., 2015), but this is understudied.

The most active and least understood component of the soil C cycle is DOC, which is part of the broader dissolved organic matter (DOM) pool. Suboxic/anoxic conditions in flooded paddy soils result in higher concentrations of DOC than in oxic soils. It is thought that DOM serves as the substrate for both greenhouse gas (CO_2 and CH_4) production and SOC formation (Bertora et al., 2020; Kalbitz et al., 2000; Kögel-Knabner et al., 2010). Different soils and residues produce DOM with varying lability and stability (Kalbitz et al., 2003). Rice residues seem relatively recalcitrant (Zhu et al., 2017) but contribute more to the DOM pool in soils with low SOC content (Ye and Horwath, 2017). It is, therefore, important to understand how soil management affects DOM chemistry.

Dissolved organic matter consists of complex structures with various functional groups, which leads to a great diversity of molecules. A subset of DOM molecules actively absorb light (chromophoric DOM; CDOM), and a subset of these molecules also fluoresce light (fluorescent DOM; FDOM) (Coble et al., 2014; Li and Hur, 2017). UV–visible spectroscopy measures light absorption by CDOM from ~250 to 700 nm. Through comparison to more sophisticated techniques such as ^{13}C-NMR, certain portions of the absorption spectrum have been shown to indicate DOM chemical makeup (Li and Hur, 2017). This includes the specific absorbance at 254 nm divided by DOC concentration ($SUVA_{254}$) which is correlated to aromaticity (Traina et al., 1990; Weishaar et al., 2003), spectral slope from 275 to 295 nm ($S_{275\text{-}295}$) and slope ratio (S_R) which are inversely correlated to molecular weight or lignin character of DOM (Helms et al., 2008), and absorption ratio at 250 nm/365 nm (E2/E3) which is inversely correlated to molecular weight and aromaticity (Li and Hur, 2017; Peuravuori and Pihlaja, 1997). Developments in UV–visible spectroscopy have allowed the simultaneous collection of absorption and fluorescence data to measure FDOM. These data can be processed into excitation-emission matrices (EEMs) that can give further insight into DOM chemistry, source, and structure (Coble et al., 1993, 2014; Cory and McKnight, 2005; McKay, 2020; Murphy et al., 2014; Stedmon and Bro, 2008). Importantly, these techniques avoid chemical alterations due to pretreatment found in fulvic/humic acid analysis. UV–visible absorption spectroscopy and especially EEMs have yet to be explored thoroughly for characterizing DOM in paddy soil.

To address these knowledge gaps, we conducted a field mesocosm and greenhouse pot study to understand how rice husk amendments with and without pretreatment affect SOC preservation, greenhouse gas emission, and DOM chemistry in a highly weathered Ultisol paddy soil. We hypothesized that: 1) Untreated rice husk amendment will increase C in SOC more than it will increase CH_4 emissions; 2) Pyrolyzed and combusted husk will not increase greenhouse gas emissions relative to control; 3) CH_4 and N_2O emissions will trade-off with Eh and global warming potential (GWP) will be minimized under AWD water management; and 4) Pyrolyzed and combusted husk amendments will produce DOM that is more aromatic/humic in nature.

2. Materials and methods

2.1. Amendment characterization

Three rice husk amendments were investigated in this study. Untreated husk ("Husk") and husk incinerated at high (>1000 °C) temperatures ("CharSil") were collected from Riceland Mills in Stuttgart, AR, USA. Rice husk biochar ("Biochar") was produced from the untreated husk in a pyrolysis oven at 450 °C, as described previously (Linam et al., 2021). Briefly, the husk was packed into air-limiting steel canisters and pyrolyzed in an oven held at 450 °C for 39 min. Canisters were removed from the oven, sealed, and allowed to cool. In this manuscript, lowercase terms (*e.g.*, "husk" and "biochar") will refer to general materials, while capitalized terms (*e.g.*, "Husk" and "Biochar") will refer to our amendments and treatments.

To determine their elemental composition, amendments were ground and digested with concentrated HNO_3 in Teflon vessels using a microwave digester (MARS6 Xpress, CEM Corporation) following previously established procedures (Seyfferth et al., 2016). These digests were analyzed via ICP-MS to determine potassium (K) and phosphorus (P) concentration in the amendments. The acid-insoluble, Si-gel fraction was centrifuged and washed before being dissolved in 2 M NaOH; Si concentration was then determined via the molybdenum blue method (Kraska and Breitenbeck, 2010). A series of standard spikes were performed on these extracts to account for interference from dark carbonized residues in the Biochar and CharSil samples. The concentrations of C and N in the amendments were determined via CHN combustion analysis (Vario Cube, Elementar).

2.2. Experimental design

2.2.1. Mesocosm study

Twelve rice paddy mesocosms ("Paddies") were established on the University of Delaware farm in Newark, DE, USA. The field had been used as an orchard ~60 years before but had been a grassland for at least 8 years prior. The paddies are 2 × 2 m with 1 m depth and are underlain by reinforced polyethylene membrane (0.6 mm thick). The paddies were backfilled with native soil, an Elsinboro silty clay loam, classified as an Ultisol/Acrisol. Rice was cultivated in the paddies for one year before the beginning of the experiment to establish paddy soil conditions. The

soil initially had 1.38% SOM measured by loss on ignition (LOI).

Before planting in 2019, the paddies were amended with one of four treatments: no amendment ("Control"), 4.92 kg (14.7 Mg/ha) Husk, 2.28 kg (6.8 Mg/ha) Biochar, or 1.41 kg (4.2 Mg/ha) CharSil, in triplicate. These rates were chosen to supply 1 Mg Si/ha in order to test the effectiveness of the amendments as Si fertilizers. This rate corresponds to returning the husk from approximately 7 years of rice production. Rice straw harvested the previous year was also returned to the paddies each spring at a rate of ~3 Mg ha^{-1} y^{-1}. Each year, the paddies were fertilized according to soil test recommendations with ~190 kg N/ha (as urea) and ~35 kg K/ha (as KCl) pre-plant, with an additional ~34 kg N/ha at booting. Hybrid rice (*Oryza sativa* L. cv CLXL745) was grown in the paddies at a planting density of 12.25 plants/m^2 each summer for three years (2019–2021). Paddies were irrigated according to safe alternate wetting and drying (AWD) practice, where they were flooded from one month post-transplant until harvest, with 1–2 midseason dry downs to 15 cm (Bouman et al., 2007; Carrijo et al., 2017). Husk, Biochar, and CharSil amendments were only added at the beginning of year 1. Plants were harvested manually at physiological maturity 108–115 days after transplanting.

2.2.2. Pot study

A pot study was conducted using soil collected from the A horizon (0–20 cm depth) adjacent to the paddy mesocosms. Rice straw (1.1 kg m^{-2}) was mixed with 8 kg (dry weight) of soil in 8 L HDPE pots, and the soils were flooded for 31 days before beginning the experiment. The 3-fold higher straw amendment rate and monthlong flood were used to establish wetland soil conditions similar to the paddy soil because the soil had previously been freely draining. The pots were then drained, and Husk (45 g), Biochar (18.5 g), and CharSil (17.4 g) amendments, along with recommended levels of N and K fertilizers, were incorporated into the soils. These husk amendment rates are similar to those used in the mesocosm study (~1 Mg Si/ha). Control pots received no husk amendment. Water management was used as an additional experimental parameter with Nonflooded (NF; soils watered twice weekly to 80% water-filled pore space and allowed to drain), alternate wetting and drying (AWD; soils flooded but allowed to drain 4 times during vegetative growth to 25% volumetric water content) and Flooded (F; soils maintained with standing water) treatments. Each treatment was repeated in triplicate for a total of 36 pots. Pots were irrigated with reverse osmosis water. Hybrid rice (*Oryza sativa* L. cv CLXL745) seedlings were then transplanted into the soils, and the plants were grown to physiological maturity in a climate-controlled growth chamber at 60% humidity with daytime temperatures of 28 °C, nighttime temperatures of 26 °C, and 14 h days with light supplied by LED LumiGro LumiBars. Further description of the experimental design can be found in a previous publication that described the amendment effects on plant and porewater inorganic chemistry (Linam et al., 2022).

2.3. Soil sampling

Soil samples were collected 9 times during the 3-year paddy mesocosm study using a 5.7 cm diameter hand corer to 15 cm depth. Two cores were composited from opposing sides of the mesocosms for each sample. The first sample was collected during the fallow period before amending the soils. Samples were also collected at harvest each year and at 1–2 points during each growing season. For the pot study, soil samples were collected before amendment and after plant harvest using a 3.8 cm diameter hand corer to a depth of 20 cm (i.e., the entire pot depth).

Soil samples were air-dried, ground to pass a 2-mm sieve, and undecomposed plant matter was removed manually. SOM content was determined using the loss on ignition method. For this, approximately 2 cm^3 of soil was added to pre-combusted beakers, dried at 150 °C for 2 h, weighed, combusted at 360 °C for 4 h, weighed again, and SOM was calculated as the difference between the weights before and after combustion. Three technical replicates were analyzed and averaged to obtain a single value for each sample. For C budget calculations, SOM values were converted to SOC by multiplying by 0.58, as is widely done (Abella and Zimmer, 2007).

2.4. Gas flux measurements

Fluxes of greenhouse gases from the paddies and pots were measured throughout the experiments using the closed chamber technique with a Gasmet DX4040 multigas analyzer (Gasmet Technologies, Vantaa, FI). For the paddies, a 2 × 2x2 m polyethylene airtight and semitransparent chamber was placed over the entirety of each paddy on the soil surface, fans were used to mix the air, and PTFE tubing was used to draw air into and return air from the instrument. Concentrations of CH_4, CO_2, and N_2O were measured for 5 min, with a 5-s integration time per point. The chamber was then removed and re-equilibrated with the atmosphere before measuring the next paddy. For the pot study, a similar procedure was performed but using a 0.045 m^3 opaque PVC headspace chamber equipped with a fan (Teasley et al., 2017), and measurement was only performed for 3 min. Gas flux measurements were taken every week during plant growth.

Analysis of gas flux data was performed using Matlab (Mathworks), with code written in-house. Linear fits of concentration vs. time were calculated for each sample, and the slope of this line was converted to a flux using soil area, air volume measured, and the ideal gas law (Limmer et al., 2018). Only data with fits having significant ($p < 0.05$) slopes were used for analysis. Global warming potential (GWP) was calculated in terms of kg CO_2 equivalents by scaling CH_4 and N_2O emissions by factors of 34 and 298, respectively (Myhre et al., 2013), and adding them to CO_2 emission. Due to the partial transparency of the chamber, plants in the paddy experiment could photosynthesize during measurement; for this reason, CO_2 flux measurements from the paddy experiment are not reported.

The carbon lost during Biochar production was assumed to be CO_2 and was calculated using Equation (1) to adjust the total GHG emissions. The C lost during CharSil production is slightly more uncertain because masses of husk and CharSil were not measured at the production facility, so Si content was used to estimate mass loss (Equation (2)); this result was then used in Equation (1) to calculate CO_2 emission during CharSil production.

$$kg\ C\ (CO_2) = \%C_{Husk} - \%C_{Biochar}\left(\frac{kg\ Biochar}{kg\ Husk}\right) \quad (1)$$

$$\frac{kg\ Charsil}{kg\ Husk} = \frac{\%Si_{Husk}}{\%Si_{CharSil}} \quad (2)$$

2.5. Porewater sampling

Soil porewater was sampled weekly in the paddy experiment and every other week in the pot study. Rhizon samplers (Rhizosphere Research Products) with a pore size of 0.15 μm were inserted at a 45° angle to sample a depth of 2–9 cm according to previous methods (Seyfferth et al., 2016; Seyfferth and Fendorf, 2012). Syringes were used to flush the Rhizons by withdrawing 5–10 mL of porewater which was discarded, then porewater (10–20 mL) was collected into HDPE bottles (paddy experiment) or combusted glass vials (pot study) both sealed anoxically and under vacuum. Vials were then opened, and a portion of the sample was acidified to 2% HNO_3 for DOC analysis via high-temperature catalytic oxidation (HTCO) using a total organic carbon (TOC) analyzer (Vario TOC Cube), along with blanks. Porewater pH and Eh were measured using calibrated electrodes (Eh calibrated against standard hydrogen electrode as ORP).

2.6. Dissolved organic matter characterization

DOM characterization was performed in the pot study to determine

CDOM and FDOM properties. Immediately after uncapping the vacuum vials, 3 drops of porewater were diluted to 7 mL using ultra-high purity 18.2 MΩ cm^{-1} H_2O (~60-fold dilution). Blanks were processed similarly with Rhizons in ultra-high purity water. All samples were stored in the dark at 4 °C until analysis. UV–visible absorbance spectra were measured, and fluorescence EEMs were generated simultaneously using an Aqualog spectrometer (Horiba). It should be noted that some samples were analyzed within a day of collection, while others were stored for up to 6 months before analysis due to COVID-19 pandemic restrictions in the spring and summer of 2020. Storage time was not a significant predictor in multiple linear regression models of EEMs component loadings, suggesting sample degradation did not affect the results of parallel factor analysis (PARAFAC). Absorption values were converted to an absorption coefficient (α) using Equation (3):

$$\alpha = A_\lambda / l \quad (3)$$

where A_λ is the absorbance at a given wavelength (λ) and l = path length (0.01 m). UV–visible data was analyzed for the parameters shown in Table 2, which broadly represent DOM aromaticity ($SUVA_{254}$ and E2/E3), molecular weight ($S_{275\text{-}295}$ and S_R; Fig. S2), or freshness (BIX).

Fluorescence intensities were measured at excitation wavelengths from 250 to 500 nm in 2 nm increments and emission wavelengths from 250 to 600 nm in 4.6 nm increments. Rayleigh scatter peaks were removed, and fluorescence intensities were interpolated across these regions. Outliers were removed, and the spectra were normalized to the Raman Scattering Area unit based on the spectrum of ultra-high purity water. Further processing was performed using the drEEM 0.5.1 software package (Murphy et al., 2014) for MATLAB (MathWorks), which modeled the data via parallel factor analysis (PARAFAC) using all samples from the experiment (n = 333). A 5-component model was chosen based on minimum component collinearity, minimum sample leverages, random/minimum residuals, the minimum sum of squares error, spectra resembling real fluorophores, and split half analysis as described in previous literature (Stedmon and Bro, 2008) and shown in Fig. S3. Components were compared to Coble peak locations and interpretations (Coble et al., 2014).

2.7. Mass balance calculation

Mass balances for C were calculated by comparing the SOC storage with CH_4 emission data from the paddy study and the SOC storage with CO_2 emission data from the pot study, all relative to Control treatments and converted to kg C (CO_2 equivalents) m^{-2} y^{-1}. The 3-year cumulative CH_4 emission and SOC storage values from the paddies were divided by 3, while only the single-year CO_2 values from the pot study were used. Amendments did not significantly affect N_2O emissions; therefore, these values were excluded from our calculation. It should also be noted that the differences in SOC storage and CH_4 emissions between Control and Biochar/CharSil were used in the mass balance calculation even though they were not statistically significant at α = 0.05 level.

2.8. Statistics

One- and two-way ANOVA analyses, repeated measures ANOVA, multiple linear regression (MLR), and principal component analysis (PCA) were performed using JMP Pro 16 (SAS Institute). Time-weighted averages of all relevant porewater chemistry (pH, Eh, and DOC), UV–visible ($SUVA_{254}$, E2/E3, $S_{275\text{-}295}$, and S_R), and EEMs (Components 1–5 loadings) parameters were entered as predictors in MLR models, with nonsignificant predictors removed sequentially until only significant predictors remained in the model. All measured parameters were included in the PCA model. Significance of the results was generally defined at the $p < 0.05$ level.

Table 2
Labels, formulas, interpretations, and references for the UV–visible parameters analyzed in the pot study DOM samples. A = absorption coefficient, S = slope, F = fluorescence intensity, Ex = excitation, and subscripts denote wavelength used.

Parameter	Formula	Interpretation	References
$SUVA_{254}$	$\frac{a_{254}}{DOC\ (mM)}$	Aromaticity	(Traina et al., 1990; Weishaar et al., 2003)
E2/E3	$\frac{a_{250}}{a_{365}}$	Inverse to molecular weight and aromaticity	Peuravuori and Pihlaja (1997)
$S_{275\text{-}295}$	$\left\|\frac{\ln(a_{295}) - \ln(a_{275})}{295 - 275}\right\|$	Inverse to molecular weight	(Helms et al., 2008, 2013)
S_R	$\frac{S_{275-295}}{S_{350-400}}$	Inverse to molecular weight	(Helms et al., 2008, 2013)
BIX	$\left(\frac{380_F}{430_F}\right)_{Ex=310}$	Correlated to recently produced DOM	(Huguet et al., 2009; Parlanti et al., 2000; Wilson and Xenopoulos, 2009)

3. Results

3.1. Yield and productivity

The rough rice yield ranged from 6 to 10 t ha^{-1} in the paddy study and 5–8 t ha^{-1} in the pot study (Fig. S1), with the difference in productivity likely due to inaccuracies in scaling factors. Amendments only significantly impacted the rough rice yield in the paddies, with Biochar paddies having a 9% higher yield than Control ($p < 0.01$). The rough rice and straw yields were both significantly higher in the first year of the paddy study compared to the second and third years (Fig. S1). In the pot study, AWD had 32% higher rough rice yield than Nonflooded ($p = 0.01$). In addition to Si and C, amendments contain significant amounts of N, P, and K (Table 1) and our amendment rates provided 50, 10, and 37 (Husk), 42, 10, and 30 (Biochar), and 11, 10, and 36 (CharSil) kg N, P, and K ha^{-1}, respectively.

3.2. Soil organic matter

The SOM content increased with all amendments over the three-year paddy experiment ($p < 0.001$; Fig. 1). All amendments significantly increased SOM relative to Control and Husk had significantly higher SOM than CharSil according to repeated measures ANOVA results ($p < 0.001$; Fig. 1). After three years, the SOM for all treatments had increased by 0.8–1.3%, a relative increase of 53–94%. If the Control treatment is considered a baseline, an excess of 0.11–0.30 kg C m^{-2} y^{-1}

Table 1
Carbon, nitrogen, phosphorus, potassium, and silicon content of the rice straw and husk amendments used in this study. Amount of carbon added per soil area is also shown for the paddy mesocosms and pot study.

Amendment	Carbon	Nitrogen	Phosphorus	Potassium	Silicon	Carbon	Carbon
	%	%	%	%	%	kg/m^2 paddies	kg/m^2 pots
Straw	39	0.87	0.17	2.58	3.8	0.10	0.43
Husk	40	0.34	0.07	0.25	6.8	0.49	0.44
Biochar	49	0.62	0.15	0.44	14.7	0.28	0.22
CharSil	26	0.26	0.23	0.84	23.8	0.09	0.11

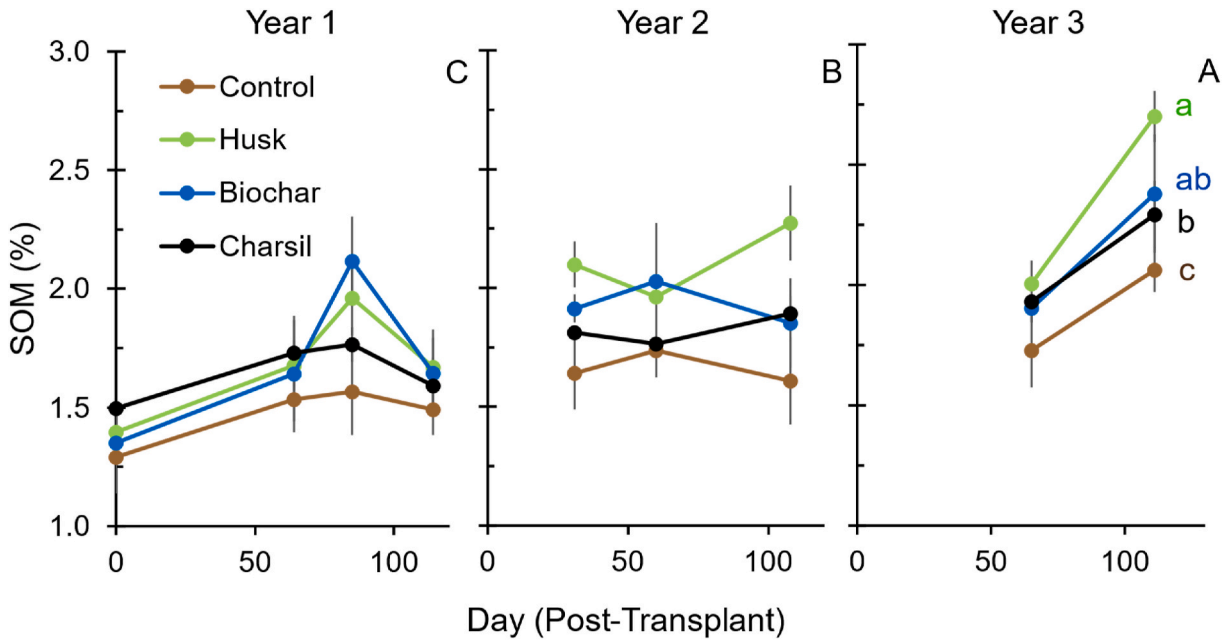

Fig. 1. Soil organic matter from the paddy mesocosms over the 3-year experiment. Color-coded lowercase letters represent repeated measures ANOVA with Tukey HSD results for amendment effects, while uppercase letters on the right of each panel represent time effects by year, showing that SOM increased each year for all treatments. Error bars represent standard deviation (n = 3; α = 0.05).

accumulated in the paddy soil due to amendments (Fig. 2). These values are 1.2–2.9 times higher than the mass of C added through amendments.

The SOM content decreased in all pot study samples by 0.15–0.61% compared to the original undisturbed soil samples analyzed before beginning the experiment. Normalizing by the final SOM in the Control treatment, all amendments increased SOM storage in Flooded pots with a similar trend (Husk > Biochar > CharSil) and magnitude (12–21% relative increase per year) to the paddy experiment (Fig. 2); these differences were not statistically significant though (p = 0.14). Water management significantly (p = 0.02) impacted SOM storage in the pot study, with Flooded treatments storing more SOM than AWD and Non-flooded treatments (Fig. 2).

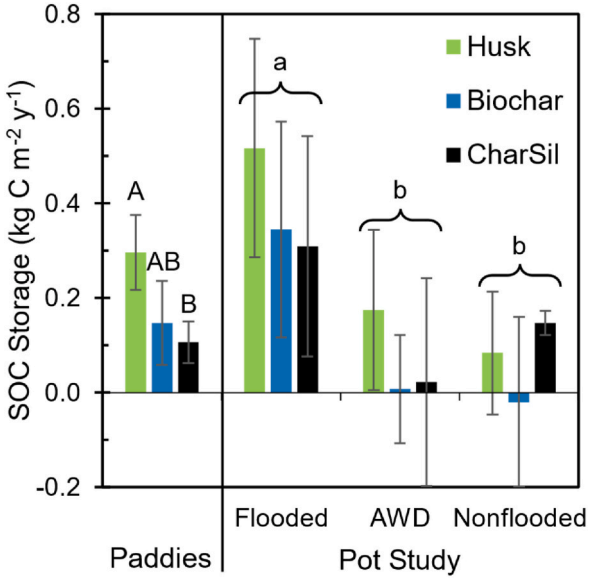

Fig. 2. Excess SOC storage normalized to Control treatments at the conclusion of the paddy (left) and pot study (right) experiments. Uppercase letters represent amendment differences from Control, while lowercase letters with brackets represent water management treatment groupings from ANOVA with Tukey post-hoc HSD tests. Statistics were calculated separately for the paddy and pot study experiments. Error bars represent standard deviation (n = 3; α = 0.05).

3.3. *Greenhouse gas emission*

Greenhouse gas (CO_2, CH_4, and N_2O) emissions varied with amendment, water management, and time. In the paddy mesocosm experiment, Husk treatments had significantly higher CH_4 emission in the first ($p < 0.01$) and second ($p = 0.02$) years of the paddy experiment, but in the third year, there were no significant differences between treatments (Fig. 3). Cumulatively, Husk amendment resulted in 54 ± 10% higher CH_4 emissions than Control ($p < 0.01$), but there were no significant differences between the Control, Biochar, and CharSil treatments. No N_2O was detected in weekly flux measurements, and CO_2 data was not reported due to photosynthesis during measurement, as described in section 2.4.

In the pot study, CH_4 emission was significantly ($p = 0.03$) higher in the Flooded compared to Nonflooded treatments but did not vary by amendment (Fig. 4a) due to large standard deviations in measurements. Emissions of N_2O showed the opposite trend, being significantly ($p < 0.01$) higher for Nonflooded compared to AWD and Flooded treatments (Fig. 4b); emission of N_2O and CH_4 were simultaneously minimized at an Eh of 250–300 mV (Fig. S4). Assuming that the C lost during Biochar and CharSil production was emitted as CO_2 (Equation (1)), there are significant water management and amendment effects on CO_2 production in the pot study (Fig. 4c). Emission of CO_2 increased significantly ($p < 0.01$) from Flooded to AWD to Nonflooded water management, and CharSil treatments had significantly ($p < 0.01$) higher CO_2 emission compared to Control, Husk, and Biochar treatments. When CH_4 and N_2O emissions are converted into global warming potentials (CO_2 equivalents), GWP follows the same trends as CO_2, with significantly ($p = 0.04$) higher GWP for Nonflooded treatment compared to Flooded, and significantly ($p = 0.02$) higher GWP for CharSil treatment compared to Control (Fig. 4d). The GWP of CO_2 in this study is higher than N_2O and CH_4 and could potentially be inflated due to the substantial decrease in SOC observed in the pot study, likely from disturbing the native soil. Whenever CO_2 is not factored into GWP, there are no significant differences in GWP between treatments.

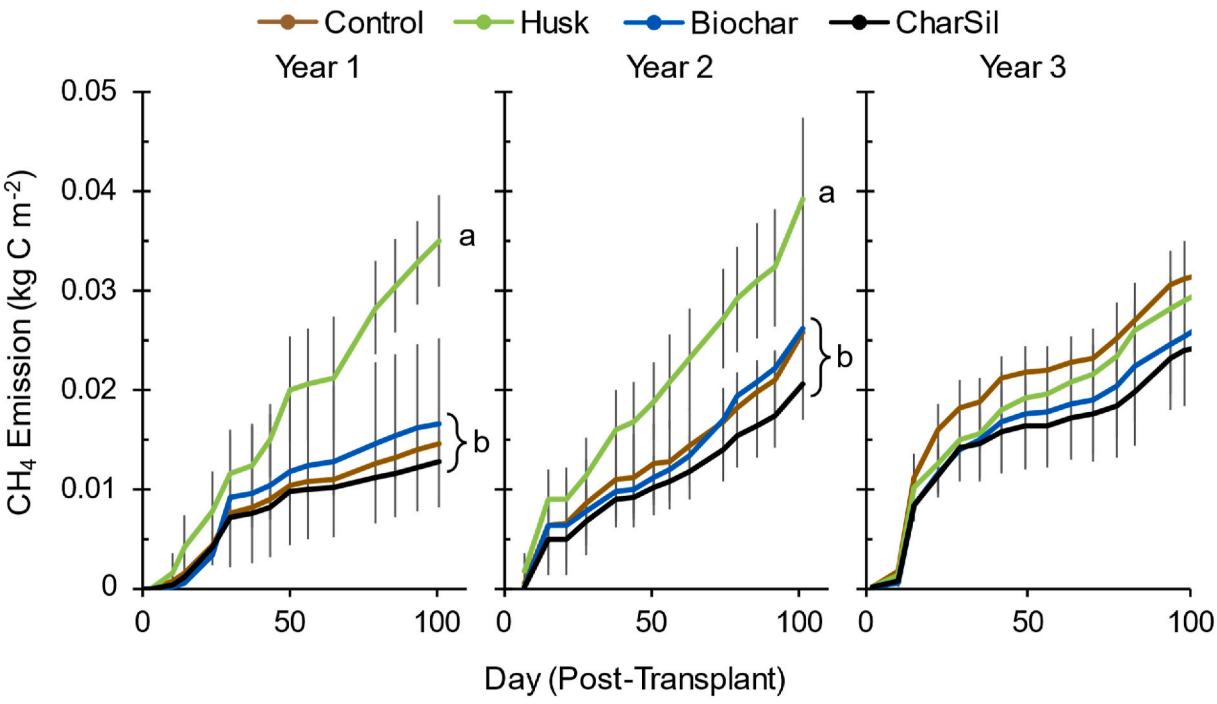

Fig. 3. Cumulative CH_4 emissions from the paddy mesocosms over the 3-year experiment. Lowercase letters represent ANOVA with Tukey HSD groupings for the end-of-year sums. Error bars represent standard deviation (n = 3; α = 0.05).

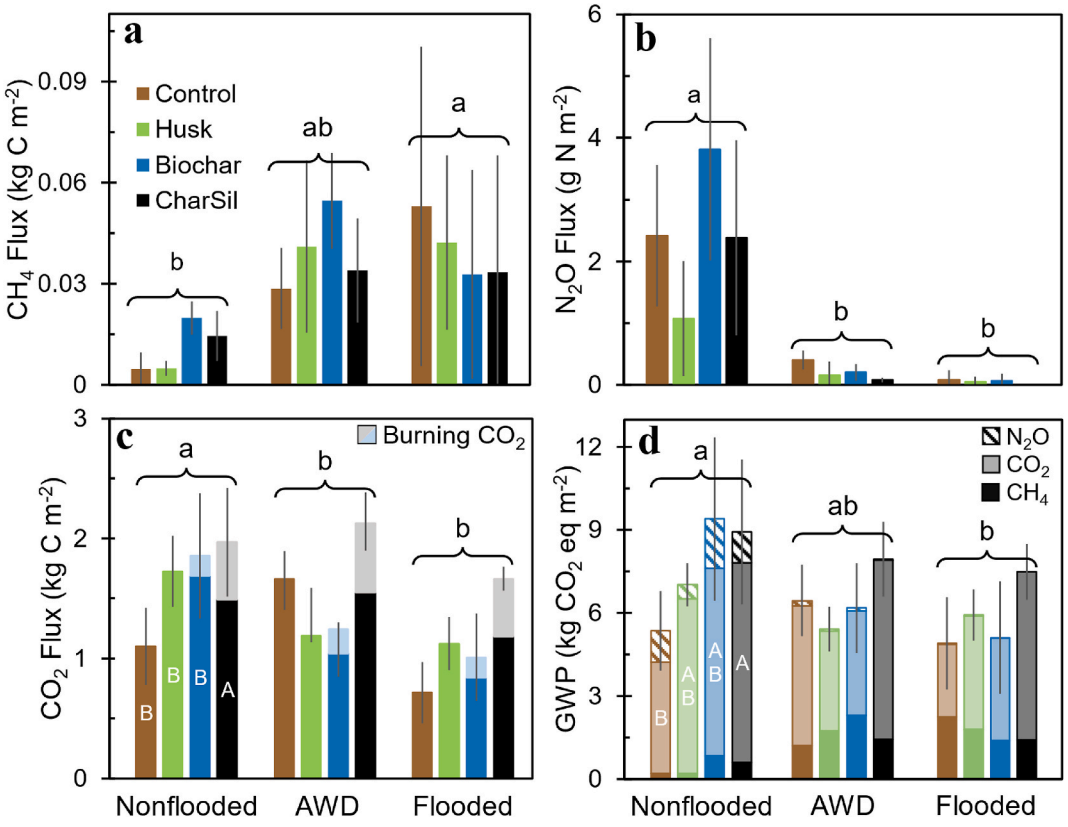

Fig. 4. Cumulative CH_4 (a), N_2O (b), CO_2 (c), and global warming potential (d) fluxes from the pot study. Lowercase letters with brackets represent Tukey HSD groupings for water management effects, and uppercase letters inside first sets of bars represent Tukey HSD groupings for amendment effects across water managements; there were no significant interaction effects. Lightly shaded sections of Biochar and CharSil bars represent CO_2 emitted during the production of amendments (c). Striped sections of bars represent N_2O contribution, lightly shaded sections represent CO_2 contribution, and fully solid sections represent CH_4 contribution to global warming potential (d). Error bars represent standard deviation (n = 3; α = 0.05).

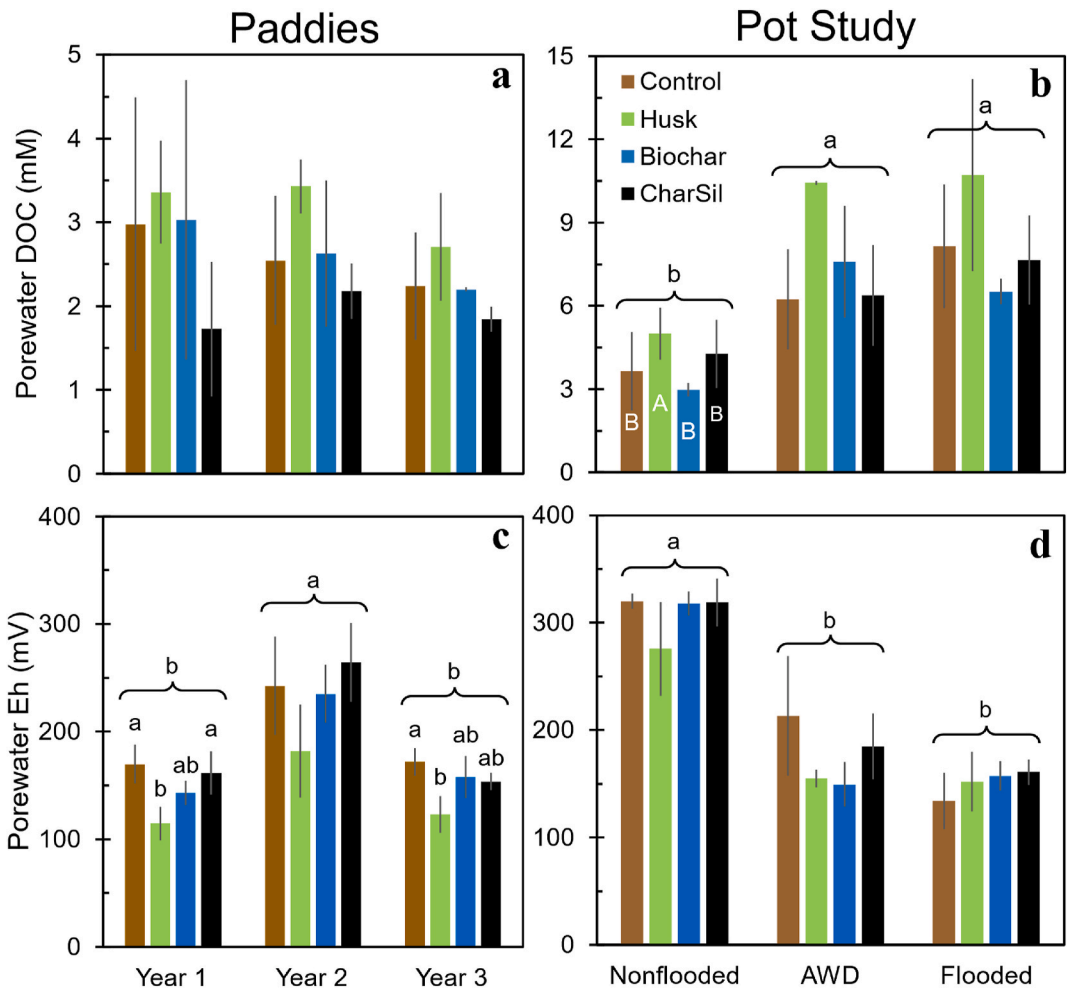

Fig. 5. Time-weighted average porewater DOC concentrations (a,b) and porewater Eh (c,d) for the paddy mesocosm (left) and pot study (right) experiments. Uppercase letters inside first set of bars in (b) represent Tukey HSD groupings for amendment effects across water managements, brackets with lowercase letters represent groupings for water management (b,d) or year (c), and lowercase letters above bars in (c) represent groupings for amendment within each year. Error bars represent standard deviation (n = 3; α = 0.05).

3.4. Dissolved organic matter chemistry

3.4.1. Dissolved organic carbon concentrations

DOC concentrations in the paddy study were not significantly affected by amendment (p = 0.18–0. 43; Fig. 5a, S5) or time (p = 0.15). Flooded soils in the pot study had significantly higher ($p < 0.01$) DOC than Nonflooded soils, and Husk amendment increased porewater DOC by 31–67% compared to Control ($p < 0.01$; Fig. 5b, S6). Porewater DOC concentrations were approximately 3-fold higher in the pot study compared to the paddy mesocosms, likely due to the higher straw amendment rates. The trend in porewater Eh is generally opposite that of DOC, with Nonflooded water management producing a significantly higher Eh ($p < 0.001$; Fig. 5d, S6) in the pot study, and Husk significantly decreasing Eh in years 1 and 3 of the paddy experiment (p = 0.015–0.02 3; Fig. 5c, S5). This suggests that the Husk amendment can provide labile C that decreases soil Eh and that Flooded conditions tend to mobilize DOC from the soil. Although the paddies were allowed to drain 2-4 times during the growing seasons (i.e., "safe" AWD), these drydowns were not as severe as in the pot study, and the porewater Eh values were more similar to the Flooded pot study treatment (~100–150 mv).

3.4.2. Dissolved organic matter chemistry

The UV–visible absorption data suggest that water management plays a dominant role in determining the chemistry of CDOM in the pot study, with amendments playing a minor role. The average porewater E2:E3, S_R, and BIX indices were significantly higher for Nonflooded treatment compared to AWD and Flooded treatments (Fig. 6b,d,e; $p < 0.01$). In contrast, the $SUVA_{254}$ value was significantly ($p < 0.01$) higher for AWD and Flooded treatments compared to Nonflooded (Fig. 6a). The amendments did not significantly alter values for any of these parameters. Average $S_{275\text{-}295}$ generally decreased as soil flooding increased (Fig. 6c) and was significantly (p = 0.01) affected by amendment × water management interactions. The results suggest that flooding increased DOM molecular weight most strongly for Control and Husk treatments, with Biochar and CharSil largely unaffected.

EEMs PARAFAC modeling was successful with this dataset (Fig. S3). The 5-component model developed explained 99.2% of the variability in our dataset, and split-half analysis validated the model using a convergence criterion of 10^{-8} as recommended (Murphy et al., 2014). Component spectra resemble real fluorophores and are shown in Fig. 7. Comparison to Coble peaks from the literature suggests that Component 1 resembles Coble C and A ("humic-like"), Component 2 resembles Coble M ("marine humic-like"), Component 3 somewhat resembles Coble D ("soil fulvic acid"), Component 4 resembles Coble T ("tryptophan/protein-like"), and Component 5 resembles Coble B ("tyrosine/-protein-like"). The primary fluorescence peak in Component 3 does not resemble any Coble peaks. Analysis of normalized component loadings shows that Component 1 is significantly ($p < 0.01$) higher in AWD and Flooded treatments compared to Nonflooded treatments, while the

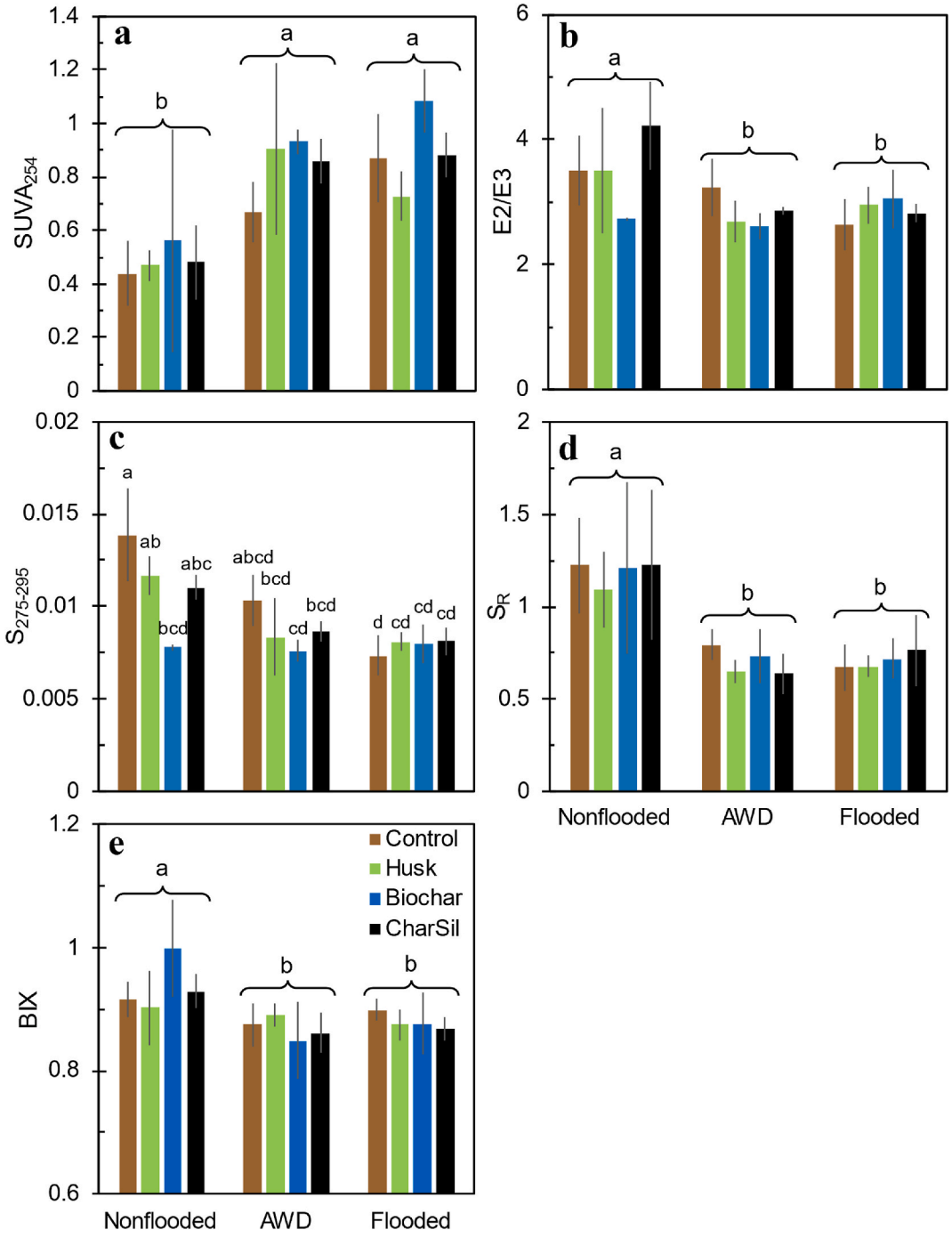

Fig. 6. Time-weighted average UV–visible absorption parameters for pot study porewater. Lowercase letters with brackets represent Tukey HSD groupings for water management effects, while lowercase letters above bars represent amendment × water management interaction effects. Error bars represent standard deviation (n = 3; α = 0.05).

reverse is true for Component 4 ($p < 0.01$), and Component 5 is significantly higher in Nonflooded treatments compared to Flooded ($p = 0.05$; Fig. S7). Amendments did not significantly impact EEMs spectra for our samples.

3.5. Pot study statistics

Principal component analysis of average soil carbon (SOM), porewater DOM (DOC, $SUVA_{254}$, E2:E3, S_R, $S_{275\text{-}295}$, EEMs components), and greenhouse gas emission (CO_2, CH_4) data from the pot study revealed the relationships between carbon components in this soil. The first two components explained 58.6% of the variability in the data (Fig. S8). Samples seem to separate on Component 1 primarily due to Eh or water management, while Component 2 somewhat discriminates between Biochar and CharSil/Husk samples. Component 3 explains 10.0% of the variability and is primarily correlated with SOM and EEMs C2 and C3 (Fig. S8).

Emission of CO_2 was best modeled using multiple linear regression with Eh (+) and S_R (−) as significant predictors ($R^2_{adj} = 0.42$, $p < 0.001$; Table S1, Fig. S9). Emission of N_2O was not correlated with DOM parameters and was best predicted by porewater Eh ($R^2 = 0.53$, $p < 0.01$; Table S1). Average porewater DOM S_R shows an exponential

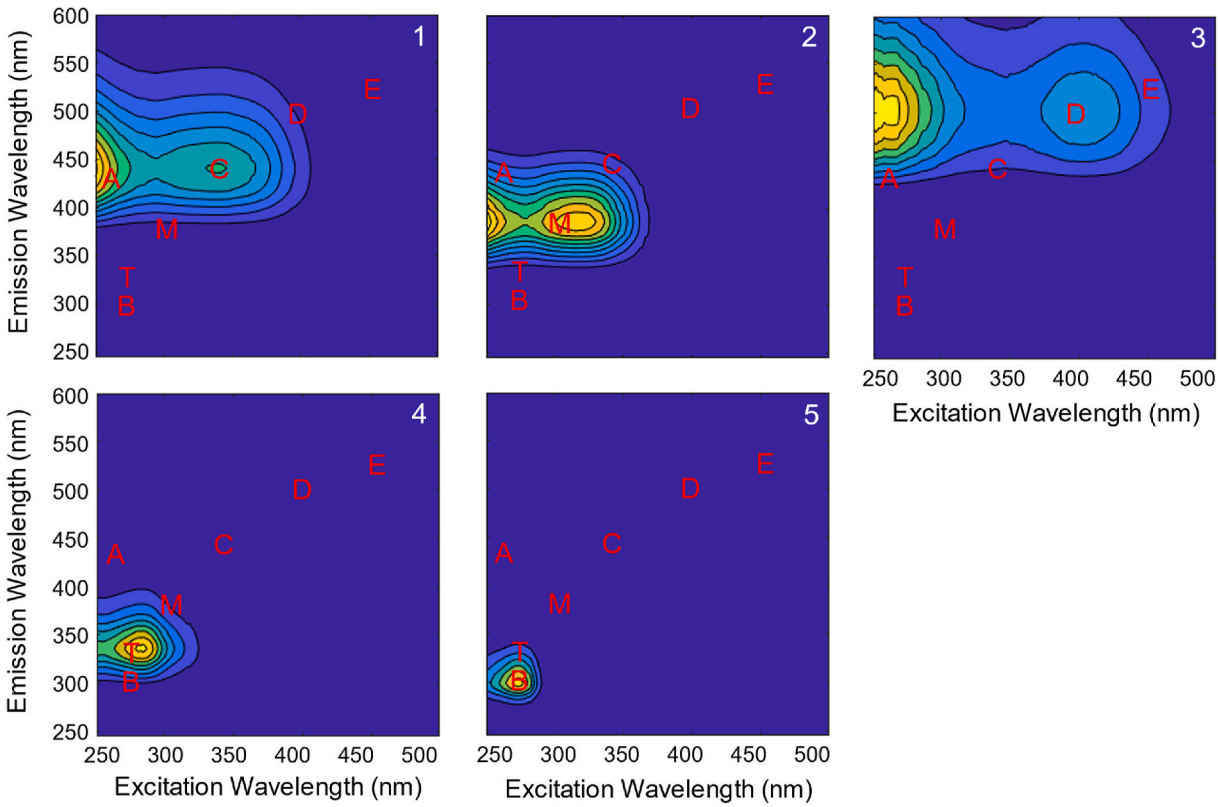

Fig. 7. EEMs fingerprint spectra for the validated 5-component PARAFAC model of all porewater samples in the pot study (n = 333). Component numbers are shown in the top right of images, emission wavelengths on the y-axis, and excitation wavelengths on the x-axis. Red letters correspond to Coble peaks.

relationship to average CH_4 emission, which explains 54% of the variability (Fig. 8); this simple model outperformed any multiple linear regression model for CH_4. All models performed significantly better for average values compared to all data points from the growing season, and therefore average values were used here. Predicted vs. average correlations and residual plots are shown in Fig. S9.

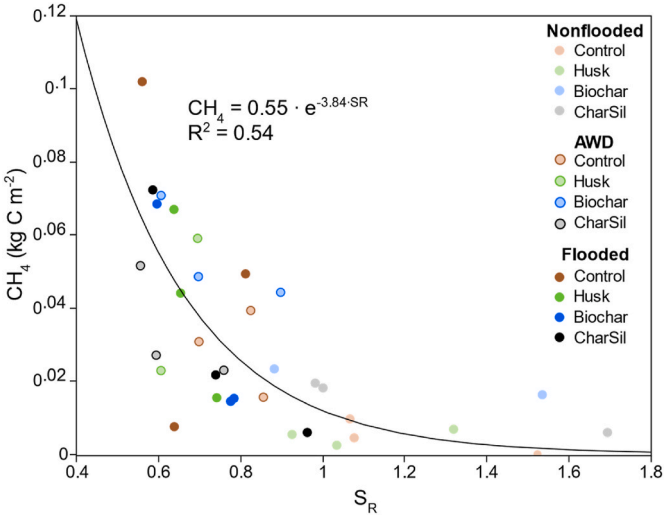

Fig. 8. Exponential relationship between average porewater DOM slope ratio (S_R) and average CH_4 emissions from the pot study. S_R was a better predictor for CH_4 emissions than Eh and/or DOC.

4. Discussion

4.1. SOC and GHG tradeoff with husk, biochar, and CharSil

Previous research has examined how rice straw management affects SOC and GHGs (Bierke et al., 2008; Bossio et al., 1999; Delwiche and Cicerone, 1993; Liu et al., 2014; Penido et al., 2016; Rahman et al., 2016; Xionghui et al., 2012; Ye and Horwath, 2017; Zhang et al., 2012), but to our knowledge, this is the first study examining how the return of rice husk contributes to the soil C cycle in rice paddies. Our data fully support our first hypothesis that the Husk amendment would cause SOC storage greater in magnitude than any increased CH_4 emission and partially supports our second hypothesis that Biochar and CharSil would not increase GHG emissions.

In the three-year paddy mesocosm study, untreated Husk amendment significantly increased CH_4 emissions by 54% but also significantly increased SOC by 1.3%. When these figures are converted into CO_2-equivalents, we observed SOC storage of 0.89 kg C m^{-2} and emission of 0.45 kg C (CH_4 as CO_2 eq.) m^{-2} over 3 years, resulting in net storage of 0.15 kg C m^{-2} y^{-1}. Biochar and CharSil significantly increased SOM by 1.0% and 0.8% compared to Control, respectively. While there were no significant differences between Biochar, CharSil, and Control CH_4 emissions, the same calculation gives similar values of 0.14 and 0.15 kg C m^{-2} y^{-1} storage for Biochar and CharSil, respectively. These data suggest that the return of husk residues, whether untreated, pyrolyzed or combusted, leads to net C storage in soil greater than any increased CH_4 emissions. Further work is necessary to validate these findings in a variety of soils.

While the CH_4 flux values were consistent across both experiments, they are quite high for all three years of the paddy (129–392 kg C ha^{-1} y^{-1}) and especially the pot study (328–530 kg C ha^{-1} y^{-1}) compared to typical CH_4 flux values measured for rice grown in California and Arkansas, USA, which are ~71–195 kg C ha^{-1} y^{-1} (Brye et al., 2016;

Runkle et al., 2019; Verfaillie et al., 2016). Our CH_4 emissions are similar in magnitude to those measured from coarser-textured paddy soils (Brye et al., 2013; Maboni et al., 2021; Martínez-Eixarch et al., 2021), which have higher gas diffusion and availability of C-rich substrates. The large CH_4 emissions and higher DOC concentration in the pot study compared to the paddy mesocosms is likely due to the higher straw amendment rate (~3x) used in the pot study.

The paddy mesocosm CO_2 data provided quasi-net ecosystem exchange, so it could not be used in estimating the loss of CO_2 via respiration; however, the pot study provided CO_2 emission data (Fig. 4) that represented soil respiration due to the use of a closed dark chamber. Therefore, we only used CO_2 emission data from the pot study for comparing CO_2 emissions by treatment. Amendments generally increased CO_2 emissions relative to Control, but this was only significant for CO_2 emissions from the Charsil amendment (Fig. 4c). Net increased CO_2 emissions were 57% (Biochar), 93% (Husk), and 424% (CharSil) relative to the amount of C added for each amendment, which suggests significant SOC mineralization priming (Miao et al., 2017), especially from CharSil. Considering the SOC and CO_2 balance, amendments of Husk and Biochar stored 0.11 and 0.05 kg C m^{-2} y^{-1} while CharSil released 0.64 kg C m^{-2} y^{-1} under flooded conditions. A limitation to this calculation is that we are not considering the CO_2 initially removed from the atmosphere when the plant produced the husk used for amendments. Therefore, our measurements overestimate the contribution of CO_2 to GWP. Finally, GHG emissions during pyrolysis (Biochar) or combustion (CharSil) of agricultural amendments are largely ignored, but our data shows that 12–42% and 33–52% of the total CO_2 emissions from Biochar and CharSil, respectively, are released during pretreatment.

Our data suggests that Husk and Biochar store more C as SOC than they emit as CH_4 or as CO_2, but there are some limitations of the C balances calculated in this study that should be considered. The primary uncertainty is due to our inability to validate our CO_2 emission data from the pot study with data from the paddy experiment. Our large straw amendment rate in the pot study was intended to acclimate the soil to flooded paddy conditions before starting the experiment. The extra straw and re-packing the soil in pots also produced high porewater DOC concentrations and overall SOC loss in the pot study, which suggests the soil was not in a steady-state when we began this experiment, likely contributing to us overestimating CO_2 emissions. Also, we only measured CO_2 emissions for one growing season in the pot study, whereas we monitored CH_4 emissions and SOC storage for 3 seasons in the paddy study. We should note that GHG emissions were not measured outside of the growing season, but previous studies suggest that emissions of CH_4 during fallow periods are substantially lower (Fitzgerald et al., 2000; Hwang et al., 2017; Koyama et al., 2015; Reba et al., 2019). Fallow periods can generate significant amounts of CO_2, which should be studied in more detail (Verfaillie et al., 2016). It should also be noted that while the trend of SOM in the pot experiment was the same as in the paddies (*e.g.* Husk > Biochar > CharSil > Control), these differences were not significant in the pot experiment and only held true for the Flooded treatment. Regardless of how CO_2 emissions are treated for GWP calculation, our data suggests that Husk, Biochar, and CharSil all store more C as SOC than they emit as CH_4 when applied to paddy soil. A long-term study measuring SOC, CH_4, and CO_2 simultaneously in both growing and fallow seasons in different soil types is necessary to determine the optimal rice husk management strategy.

4.2. Trade-off between CH_4 and N_2O emissions

Our data partially support our third hypothesis that GWP would be minimized under AWD water management. We observed a clear exponential tradeoff between CH_4 and N_2O emissions from Nonflooded to Flooded treatments in the pot study (Fig. 4, S4; Table S1). Soil Eh seems to play a key role in determining GHG flux from paddy soil, and we observed simultaneous minimization of both CH_4 and N_2O at an Eh of 250–300 mV in our soil (Fig. S4). It is also evident that our AWD treatment was not severe enough to reach this Eh region, as our paddy and pot study AWD treatments were much more similar to the pot study Flooded treatment (Fig. 5); the frequency and intensity of dry-downs are correlated with the decrease in CH_4 emissions from rice paddies under AWD water management (Balaine et al., 2019; Carrijo et al., 2018; Linquist et al., 2015). This critical Eh value is expected to differ depending on soil type and C:N ratio; however, it is centered on the same range as has been reported previously when corrections are made for electrode calibration (Yu and Patrick, 2003). Interestingly, it is also similar to the Eh that was found to minimize arsenic and cadmium uptake by rice in this soil (Linam et al., 2022), but it is unknown whether this is a broader trend that holds for other soils.

Converting the CH_4 and N_2O emissions to CO_2 equivalents illustrates that CH_4 contributes more to GWP than N_2O in this soil (Fig. S4), but Fig. 4d shows that CO_2 emissions are the largest contributor to the overall GWP. This finding corresponds with previous studies that showed CO_2 emissions contribute the most to rice paddy GWP when CO_2 removal by plants is not factored in (Gutekunst et al., 2017; Reba et al., 2019). There was also a significant water management effect on CO_2 emission in the pot study, with Flooded < AWD < Nonflooded (Fig. 4c). This has been observed in other paddy soils (Yu and Patrick, 2003) and further supports the preservation of C under flooded conditions (Fig. 2).

4.3. DOM chemistry

We reject our fourth hypothesis that Biochar and CharSil would produce DOC with more aromatic or humic character. There is little evidence from UV–visible spectroscopy or EEMs that Biochar or CharSil altered DOM chemistry, with only $S_{275\text{-}295}$ being affected by amendment × water management interactions (Fig. 6). The only clear impact of amendments on DOM was increased porewater DOC concentration due to Husk treatment in the pot study (Fig. 5). More labile C fractions (*e.g.,* water-soluble C, microbial biomass C) are thought to be more affected by organic amendments than SOC (Banger et al., 2010); however, we did not observe statistically significant impacts on porewater DOC in the paddy study (Fig. 5).

Water management played a much larger role in determining porewater DOM characteristics according to UV–visible spectroscopy and EEMs data (Fig. 6, S7). The increase in $SUVA_{254}$ and decrease in E2/E3, $S_{275\text{-}295}$, and S_R with increased flooding suggests that porewater DOM is more aromatic and has a larger average molecular weight under anoxic conditions (Bertora et al., 2020). This suggests that either reductive dissolution of iron oxides under anoxic conditions releases high molecular weight DOM that is usually strongly adsorbed in oxic conditions (Guo and Chorover, 2003), or smaller DOM molecules are preferentially degraded or used for methanogenesis in suboxic conditions, resulting in larger molecular weight DOM remaining. Higher BIX in Nonflooded conditions suggests increased microbial reworking of DOM in oxic conditions. It should be noted that E2/E3 and similar indices (*e.g.*, E4/E6) are often measured on alkali-extracted OM, and thus caution should be used for the interpretation of these values for untreated porewater. Although $S_{350\text{-}400}$ differed significantly with amendment × water management interaction effects (not shown), studies suggest it is less predictable and, therefore, less appropriate than $S_{275\text{-}295}$ and S_R for inferring DOM molecular weight (Helms et al., 2008, 2013; Yamashita et al., 2013).

Our EEMs data corroborate the UV–visible spectroscopy results, with the humic-like Component 1 being significantly higher in Flooded and AWD treatments than Nonflooded (Fig. S7). Literature from marine studies shows higher molecular weight, higher aromaticity, and humic nature of DOM molecules in oxygen-limiting conditions similar to our soils (Loginova et al., 2016; Margolin et al., 2018). Components 4 and 5 were similar to Coble peaks T and B, respectively, which have been described as protein-like DOM (Fig. 7). These components are significantly higher in Nonflooded than in Flooded treatments (Fig. S7), which suggests more microbial activity breaking down DOM in oxic conditions.

Because EEMs has not been widely applied to soils, further study is required to determine whether marine and aquatic science interpretations hold for soil environments.

Our results show promise for using UV–visible spectroscopy and EEMs data to characterize DOM in soils. Most of the variation in our C data is due to flooding/redox effects; however, slight differences in some variables (*e.g.*, SOM, $SUVA_{254}$, and EEMs C2, C3, and C5) seem to be somewhat associated with husk amendments in this study (Fig. S8). These differences were not statistically significant, which suggests several possibilities that require further investigation. First, our sample set may not have had enough variation due to using only one soil type. Successful analysis of EEMs data with PARAFAC requires a sample set with enough variation to measure real differences between samples but not so much variation that the PARAFAC model is unstable (Stedmon and Bro, 2008). We do not believe this to be problematic for our study, as we had several hundred samples measured over time and Eh gradients, and the model validation process was successful. Second, our samples could have degraded during the extended sample storage time of up to 6 months due to COVID-19 restrictions. This possibility is much more challenging to analyze, but storage time was not a significant predictor in any of our multiple linear regression models and is not strongly correlated with any UV–visible spectroscopy or EEMs parameter. Still, our conclusions should be further validated in additional studies. It is also known that ferric iron (Fe(III)) can interfere with UV–visible and EEMs spectra (Poulin et al., 2014; Weishaar et al., 2003) or can interfere by forming Fe(III) oxides which adsorb DOM, but the 60-fold dilution factor used here minimized interferences. Finally, spectroscopic methods may not be appropriate for detecting the impacts of husk amendments on soil carbon. UV–visible and EEMs analyses are untargeted methods that characterize a limited analytical window of DOM; <50% of DOM molecules absorb UV–visible light, and fluorescent yields for these molecules are only 0–3% (McKay, 2020). Previous work shows soil management or organic amendments can have a substantial (Li et al., 2019; Wu et al., 2020) or minor (Romero et al., 2019) effect on UV–visible spectroscopy and EEMs data from soil porewater. Measuring UV–visible and EEMs spectra from different soils with different management practices will show the potential of these techniques for characterizing paddy soil DOM.

4.4. Pot and field study comparison

Greenhouse and lab-scale studies simplify environmental and agricultural studies in many ways, but it is important to understand their limitations. In this study we were directly able to compare greenhouse gas emission, SOC, and DOC data from a greenhouse pot scale to a mesocosm paddy scale. Methane emission data had much higher standard deviations for the pot study than the paddy experiment (RSD = 25–104% vs. 11–23%; Fig. 4a and 3). The pot study also allowed us to use an opaque chamber and include Nonflooded treatments to obtain CO_2 and N_2O emission data. The values for SOC storage (Fig. 2) and porewater DOC (Fig. 5) were elevated in the pot study compared to the paddy experiment; we attribute this to higher straw amendment rates and the process of collecting and packing soil in pots. It is also evident that one plant growth cycle does not sufficiently capture the significant changes in SOC and CH_4 emissions seen 2–3 years after amendment (Fig. 3).

5. Conclusions

While untreated (Husk), pyrolyzed (Biochar), and combusted (CharSil) rice husk are known Si-rich amendments for rice paddies, their impacts on SOC storage, greenhouse gas emission, and DOM chemistry have not been previously investigated. In the paddy mesocosm experiment, we found that Husk, Biochar, and CharSil amendments all store more SOC than they emit as CH_4, storing a net 0.14–0.15 kg C (CO_2 eq.) $m^{-2}\ y^{-1}$ over the course of 3 years. This is despite Husk increasing CH_4 emissions. In the pot study, we found that CharSil may cause a net C release (0.64 kg C $m^{-2}\ y^{-1}$) primarily due to high CO_2 emissions during production. CH_4 and N_2O emissions traded off with porewater Eh (*i.e.*, water management) in the pot study, being simultaneously minimized at 250–300 mV; this is the same range minimizing As and Cd uptake by rice in previous work, which suggests there may be a common redox buffer controlling these processes in our soil. Nonflooded conditions decreased SOC and CH_4 emissions while increasing N_2O and CO_2 emissions in the pot study. We also found that DOM molecular weight and aromaticity decreased under Nonflooded management, and two out of five EEMs PARAFAC components differ based on water management. Slope ratio (S_R) seems to be a good predictor of CH_4 emission, and our data suggest that UV–visible spectroscopy and EEMs data have the potential to describe DOM chemistry in paddy soil porewater. Taken together, our data indicate that returning rice husk or low temperature rice husk biochar to rice paddies as a nutrient or waste management strategy can build SOC at higher rates than it increases GHG emissions. These results should be validated in different paddy soils and at larger scale.

Credit author statement

Franklin Linam: Conceptualization, Investigation, Formal Analysis, Writing – original draft preparation. Matt A. Limmer: Conceptualization, Writing – Reviewing and Editing. Alina M. Ebling: Formal Analysis, Writing – Reviewing and Editing. Angelia L. Seyfferth: Conceptualization, Writing – Reviewing and Editing, Supervision, Funding Acquisition.

Declaration of competing interest

The authors declare that they have no known competing financial interests or personal relationships that could have appeared to influence the work reported in this paper.

Data availability

Data will be made available on request.

Acknowledgments

We thank Rebekah Hanrahan, Abby Evans, John Thomas, Josh Garcia, and Paige Aldred for field assistance, Andrew Wozniak for guidance on DOM characterization, and the University of Delaware Soil Testing Laboratory for analytical assistance. This research was partially supported by USDA NIFA Grant Nos. 2018-67013–27455 and 2022-67011–36457 and by the NSF Grant No. 1930806.

Appendix A. Supplementary data

Supplementary data to this article can be found online at https://doi.org/10.1016/j.jenvman.2023.117936.

References

Abella, S.R., Zimmer, B.W., 2007. Estimating organic carbon from loss-on-ignition in northern Arizona forest soils. Soil Sci. Soc. Am. J. 71, 545–550. https://doi.org/10.2136/sssaj2006.0136.

Balaine, N., Carrijo, D.R., Adviento-Borbe, M.A., Linquist, B., 2019. Greenhouse gases from irrigated rice systems under varying severity of alternate-wetting and drying irrigation. Soil Sci. Soc. Am. J. 83, 1533–1541. https://doi.org/10.2136/sssaj2019.04.0113.

Banger, K., Toor, G.S., Biswas, A., Sidhu, S.S., Sudhir, K., 2010. Soil organic carbon fractions after 16-years of applications of fertilizers and organic manure in a Typic Rhodalfs in semi-arid tropics. Nutrient Cycl. Agroecosyst. 86, 391–399. https://doi.org/10.1007/s10705-009-9301-8.

Banker, B.C., Kludze, H., Alford, D.P., DeLaune, R.D., Lindau, C.W., 1995. Methane sources and sinks in paddy rice soils: relationship to emissions. Agric. Ecosyst. Environ. 53, 243–251. https://doi.org/10.1016/0167-8809(94)00578-3.

Bertora, C., Moretti, B., Peyron, M., Pelissetti, S., Lerda, C., Said-Pullicino, D., Milan, M., Fogliatto, S., Vidotto, F., Celi, L., Sacco, D., 2020. Carbon input management in temperate rice paddies: implications for methane emissions and crop response. Ital. J. Agron. 15, 144–155. https://doi.org/10.4081/ija.2020.1607.

Bierke, A., Kaiser, K., Guggenberger, G., 2008. Crop residue management effects on organic matter in paddy soils - the lignin component. Geoderma 146, 48–57. https://doi.org/10.1016/j.geoderma.2008.05.004.

Bossio, D.A., Horwath, W.R., Mutters, R.G., Van Kessel, C., 1999. Methane pool and flux dynamics in a rice field following straw incorporation. Soil Biol. Biochem. 31, 1313–1322. https://doi.org/10.1016/S0038-0717(99)00050-4.

Bouman, B.M., Lampayan, R.M., Tuong, T.P., 2007. Water Management in Irrigated Rice: Coping with Water Scarcity. International Rice Research Institute, Los Baños, Philippines. International Rice Research Institute.

Brye, K.R., McMullen, R.L., Silveira, M.L., Motschenbacher, J.M.D., Smith, S.F., Gbur, E. E., Helton, M.L., 2016. Environmental controls on soil respiration across a southern US climate gradient: a meta-analysis. Geoderma Reg 7, 110–119. https://doi.org/10.1016/j.geodrs.2016.02.005.

Brye, K.R., Rogers, C.W., Smartt, A.D., Norman, R.J., 2013. Soil texture effects on methane emissions from direct-seeded, delayed-flood rice production in Arkansas. Soil Sci. 178, 519–529. https://doi.org/10.1097/SS.0000000000000020.

Carrijo, D.R., Akbar, N., Reis, A.F.B., Li, C., Gaudin, A.C.M., Parikh, S.J., Green, P.G., Linquist, B.A., 2018. Impacts of variable soil drying in alternate wetting and drying rice systems on yields, grain arsenic concentration and soil moisture dynamics. Field Crop. Res. 222, 101–110. https://doi.org/10.1016/j.fcr.2018.02.026.

Carrijo, D.R., Lundy, M.E., Linquist, B.A., 2017. Rice yields and water use under alternate wetting and drying irrigation: a meta-analysis. Field Crop. Res. 203, 173–180. https://doi.org/10.1016/j.fcr.2016.12.002.

Chen, X., Liu, M., Kuzyakov, Y., Li, W., Liu, J., Jiang, C., Wu, M., Li, Z., 2018. Incorporation of rice straw carbon into dissolved organic matter and microbial biomass along a 100-year paddy soil chronosequence. Appl. Soil Ecol. 130, 84–90. https://doi.org/10.1016/j.apsoil.2018.06.004.

Coble, P.G., Lead, J., Baker, A., Reynolds, D.M., Spencer, R.G.M., 2014. Aquatic Organic Matter Fluorescence. Cambridge University Press, New York, NY. https://doi.org/10.1017/CBO9781107415324.004.

Coble, P.G., Schultz, C.A., Mopper, K., 1993. Fluorescence contouring analysis of DOC intercalibration experiment samples: a comparison of techniques. Mar. Chem. 41, 173–178. https://doi.org/10.1016/0304-4203(93)90116-6.

Cory, R.M., McKnight, D.M., 2005. Fluorescence spectroscopy reveals ubiquitous presence of oxidized and reduced quinones in dissolved organic matter. Environ. Sci. Technol. 39, 8142–8149. https://doi.org/10.1021/es0506962.

Delwiche, C.C., Cicerone, R.J., 1993. Factors affecting methane production under rice. Global Biogeochem. Cycles 7, 143–155.

Denman, K.L., Brasseur, G., Chidthaisong, A., Ciais, P., Cox, P.M., Dickinson, R.E., Hauglustaine, D., Heinze, C., Holland, E., Jacob, D., Lohmann, U., Ramachandran, S., Dias, P.L. da S., Wofsy, S.C., Zhang, X., 2007. Couplings between changes in the climate system and biogeochemistry. In: Solomon, S., Qin, D., Manning, M., Chen, Z., Marquis, M., Averyt, K.B., M.T, H.L.M (Eds.), Climate Change 2007: the Physical Science Basis. Contribution of Working Group I to the Fourth Assessment Report of the Intergovernmental Panel on Climate Change. Cambridge University Press, Cambridge, United Kingdom and New York, NY, USA, pp. 499–587.

Fitzgerald, G.J., Scow, K.M., Hill, J.E., 2000. Fallow season straw and water management effects on methane emissions in California rice. Global Biogeochem. Cycles 14, 767–776. https://doi.org/10.1029/2000GB001259.

Guo, M., Chorover, J., 2003. Transport and fractionation of dissolved organic matter in soil columns. Soil Sci. 168, 108–118. https://doi.org/10.1097/01.ss.0000055306.23789.65.

Gutekunst, M.Y., Vargas, R., Seyfferth, A.L., 2017. Impacts of soil incorporation of pre-incubated silica-rich rice residue on soil biogeochemistry and greenhouse gas fluxes under flooding and drying. Sci. Total Environ. 593–594, 134–143. https://doi.org/10.1016/j.scitotenv.2017.03.097.

Haefele, S.M., Konboon, Y., Wongboon, W., Amarante, S., Maarifat, A.A., Pfeiffer, E.M., Knoblauch, C., 2011. Effects and fate of biochar from rice residues in rice-based systems. Field Crop. Res. 121, 430–440. https://doi.org/10.1016/j.fcr.2011.01.014.

Helms, J.R., Stubbins, A., Perdue, E.M., Green, N.W., Chen, H., Mopper, K., 2013. Photochemical bleaching of oceanic dissolved organic matter and its effect on absorption spectral slope and fluorescence. Mar. Chem. 155, 81–91. https://doi.org/10.1016/j.marchem.2013.05.015.

Helms, J.R., Stubbins, A., Ritchie, J.D., Minor, E.C., Kieber, D.J., Mopper, K., 2008. Absorption spectral slopes and slope ratios as indicators of molecular weight, source, and photobleaching of chromophoric dissolved organic matter. Limnol. Oceanogr. 53, 955–969. https://doi.org/10.4319/lo.2009.54.3.1023.

Huguet, A., Vacher, L., Relexans, S., Saubusse, S., Froidefond, J.M., Parlanti, E., 2009. Properties of fluorescent dissolved organic matter in the Gironde Estuary. Org. Geochem. 40, 706–719. https://doi.org/10.1016/j.orggeochem.2009.03.002.

Hwang, H.Y., Kim, G.W., Kim, S.Y., Mozammel Haque, M., Khan, M.I., Kim, P.J., 2017. Effect of cover cropping on the net global warming potential of rice paddy soil. Geoderma 292, 49–58. https://doi.org/10.1016/j.geoderma.2017.01.001.

Kalbitz, K., Kaiser, K., Fiedler, S., Kölbl, A., Amelung, W., Bräuer, T., Cao, Z., Don, A., Grootes, P., Jahn, R., Schwark, L., Vogelsang, V., Wissing, L., Kögel-Knabner, I., 2013. The carbon count of 2000 years of rice cultivation. Global Change Biol. 19, 1107–1113. https://doi.org/10.1111/gcb.12080.

Kalbitz, K., Schmerwitz, J., Schwesig, D., Matzner, E., 2003. Biodegradation of soil-derived dissolved organic matter as related to its properties. Geoderma 113, 273–291. https://doi.org/10.1016/S0016-7061(02)00365-8.

Kalbitz, K., Solinger, S., Park, J.H., Michalzik, B., Matzner, E., 2000. Controls on the dynamics of dissolved organic matter in soils: a review. Soil Sci. 165, 277–304. https://doi.org/10.1097/00010694-200004000-00001.

Khalil, M.A., Shearer, M., Butenhoff, C., Xiong, Z., Rasmussen, R., Xu, L., Xing, G., 2009. Emissions Of Greenhouse Gases From Rice Agriculture (Report No. DOE/ER/63913-1). USDOE Office of Science doi:10.2172/959124.

Kludze, H.K., DeLaune, R.D., Patrick, W.H., 1993. Aerenchyma Formation and methane and oxygen exchange in rice. Soil Sci. Soc. Am. J. 57, 386–391. https://doi.org/10.2136/sssaj1993.03615995005700020017x.

Kögel-Knabner, I., Amelung, W., Cao, Z., Fiedler, S., Frenzel, P., Jahn, R., Kalbitz, K., Kölbl, A., Schloter, M., 2010. Biogeochemistry of paddy soils. Geoderma 157, 1–14. https://doi.org/10.1016/j.geoderma.2010.03.009.

Koyama, S., Hayashi, H., 2017. Rice yield and soil carbon dynamics over three years of applying rice husk charcoal to an Andosol paddy field. Plant Prod. Sci. 20, 176–182. https://doi.org/10.1080/1343943X.2017.1290506.

Koyama, S., Inazaki, F., Minamikawa, K., Kato, M., Hayashi, H., 2015. Increase in soil carbon sequestration using rice husk charcoal without stimulating CH4 and N2O emissions in an Andosol paddy field in Japan. Soil Sci. Plant Nutr. 61, 873–884. https://doi.org/10.1080/00380768.2015.1065511.

Koyama, S., Katagiri, T., Minamikawa, K., Kato, M., Hayashi, H., 2016. Effects of rice husk charcoal application on rice yield, methane emission, and soil carbon sequestration in andosol paddy soil. JARQ (Jpn. Agric. Res. Q.) 50, 319–327. https://doi.org/10.6090/jarq.50.319.

Kraska, J.E., Breitenbeck, G.A., 2010. Simple, robust method for quantifying silicon in plant tissue. Commun. Soil Sci. Plant Anal. 41, 2075–2085. https://doi.org/10.1080/00103624.2010.498537.

Lal, R., 2004. Soil carbon sequestration impacts on global climate change and food security. Science 84 304, 1623–1627. https://doi.org/10.1126/science.1097396.

Lehndorff, E., Houtermans, M., Winkler, P., Kaiser, K., Kölbl, A., Romani, M., Said-Pullicino, D., Utami, S.R., Zhang, G.L., Cao, Z.H., Mikutta, R., Guggenberger, G., Amelung, W., 2016. Black carbon and black nitrogen storage under long-term paddy and non-paddy management in major reference soil groups. Geoderma 284, 214–225. https://doi.org/10.1016/j.geoderma.2016.08.026.

Li, M., Drosos, M., Hu, H., He, X., Wang, G., Zhang, H., Hu, Z., Xi, B., 2019. Organic amendments affect dissolved organic matter composition and mercury dissolution in pore waters of mercury-polluted paddy soil. Chemosphere 232, 356–365. https://doi.org/10.1016/j.chemosphere.2019.05.234.

Li, P., Hur, J., 2017. Utilization of UV-Vis spectroscopy and related data analyses for dissolved organic matter (DOM) studies: a review. Crit. Rev. Environ. Sci. Technol. 47, 131–154. https://doi.org/10.1080/10643389.2017.1309186.

Limmer, M.A., Mann, J., Amaral, D.C., Vargas, R., Seyfferth, A.L., 2018. Silicon-rich amendments in rice paddies: effects on arsenic uptake and biogeochemistry. Sci. Total Environ. 624, 1360–1368. https://doi.org/10.1016/j.scitotenv.2017.12.207.

Linam, F., Limmer, M.A., Tappero, R., Seyfferth, A.L., 2022. Rice husk and charred husk amendments increase porewater and plant Si but water management determines grain as and Cd concentration. Plant Soil. https://doi.org/10.1007/s11104-022-05350-3.

Linam, F., McCoach, K., Limmer, M.A., Seyfferth, A.L., 2021. Contrasting effects of rice husk pyrolysis temperature on silicon dissolution and retention of cadmium (Cd) and dimethylarsinic acid (DMA). Sci. Total Environ. 765 https://doi.org/10.1016/j.scitotenv.2020.144428.

Linquist, B.A., Anders, M.M., Adviento-Borbe, M.A.A., Chaney, R.L., Nalley, L.L., da Rosa, E.F.F., van Kessel, C., 2015. Reducing greenhouse gas emissions, water use, and grain arsenic levels in rice systems. Global Change Biol. 21, 407–417. https://doi.org/10.1111/gcb.12701.

Liu, C., Lu, M., Cui, J., Li, B., Fang, C., 2014. Effects of straw carbon input on carbon dynamics in agricultural soils: a meta-analysis. Global Change Biol. 20, 1366–1381. https://doi.org/10.1111/gcb.12517.

Loginova, A.N., Thomsen, S., Engel, A., 2016. Chromophoric and fluorescent dissolved organic matter in and above the oxygen minimum zone off Peru. J. Geophys. Res. Ocean. 7973–7990. https://doi.org/10.1002/2016JC011906 (Received).

Maboni, C., Bremm, T., Aguiar, L.J.G., Scivittaro, W.B., Souza, V. de A., Zimermann, H. R., Teichrieb, C.A., de Oliveira, P.E.S., Herdies, D.L., Degrazia, G.A., Roberti, D.R., 2021. The fallow period plays an important role in annual CH4 emission in a rice paddy in Southern Brazil. Sustain. Times 13. https://doi.org/10.3390/su132011336.

Margolin, A.R., Gonnelli, M., Hansell, D.A., Santinelli, C., 2018. Black Sea dissolved organic matter dynamics: insights from optical analyses. Limnol. Oceanogr. 63, 1425–1443. https://doi.org/10.1002/lno.10791.

Martínez-Eixarch, M., Alcaraz, C., Viñas, M., Noguerol, J., Aranda, X., Prenafeta-Boldú, F.X., Català-Forner, M., Fennessy, M.S., Ibáñez, C., 2021. The main drivers of methane emissions differ in the growing and flooded fallow seasons in Mediterranean rice fields. Plant Soil 460, 211–227. https://doi.org/10.1007/s11104-020-04809-5.

McKay, G., 2020. Emerging investigator series: critical review of photophysical models for the optical and photochemical properties of dissolved organic matter. Environ. Sci. Process. Impacts. https://doi.org/10.1039/d0em00056f.

Mer, J. Le, Roger, P., Le Mer, J., 2007. Production, oxidation, emission and consumption of methane by soils: a review. Eur. J. Soil Biol. 37, 25–50. https://doi.org/10.1016/S1164-5563(01)01067-6.

Miao, S., Ye, R., Qiao, Y., Zhu-Barker, X., Doane, T.A., Horwath, W.R., 2017. The solubility of carbon inputs affects the priming of soil organic matter. Plant Soil 410, 129–138. https://doi.org/10.1007/s11104-016-2991-1.

Minami, E., Saka, S., 2005. Biomass resources present in Japan - annual quantities grown, unused and wasted. Biomass Bioenergy 29, 310–320. https://doi.org/10.1016/j.biombioe.2004.06.012.

Murphy, K.R., Stedmon, C.A., Graeber, D., Bro, R., 2014. Fluorescence spectroscopy and multi-way techniques. Anal. Methods 2–3. https://doi.org/10.1039/c3ay41160e. Ref.

Myhre, G., Shindell, D., Bréon, F.-M., Collins, W., Fuglestvedt, J., Huang, J., Koch, D., Lamarque, J.-F., Lee, D., B.M, Nakajima, T., Robock, A., Stephens, G., Takemura, T., Zhang, H., 2013. Anthropogenic and natural radiative forcing. In: Stocker, T.F., Qin, D., Plattner, G.-K., Tignor, M., Allen, S.K., Boschung, J., Nauels, A., Xia, Y., Bex, V., Midgley, P.M. (Eds.), Climate Change 2013: the Physical Science Basis. Contribution of Working Group I to the Fifth Assessment Report of the Intergovernmental Panel on Climate Change. Cambridge University Press, Cambridge, United Kingdom and New York, NY, USA, pp. 659–740.

Parlanti, E., Worz, K., Geoffroy, L., Lamotte, M., 2000. Dissolved organic matter ¯uorescence spectroscopy as a tool to estimate biological activity in a coastal zone submitted to anthropogenic inputs. Org. Geochem. 31, 1765–1781.

Paul, E.A., 2016. The nature and dynamics of soil organic matter: plant inputs, microbial transformations, and organic matter stabilization. Soil Biol. Biochem. 98, 109–126. https://doi.org/10.1016/j.soilbio.2016.04.001.

Penido, E.S., Bennett, A.J., Hanson, T.E., Seyfferth, A.L., 2016. Biogeochemical impacts of silicon-rich rice residue incorporation into flooded soils: implications for rice nutrition and cycling of arsenic. Plant Soil 399, 75–87. https://doi.org/10.1007/s11104-015-2682-3.

Peuravuori, J., Pihlaja, K., 1997. Molecular size distribution and spectroscopic properties of aquatic humic substances. Anal. Chim. Acta 337, 133–149. https://doi.org/10.1016/S0003-2670(96)00412-6.

Poulin, B.A., Ryan, J.N., Aiken, G.R., 2014. Effects of iron on optical properties of dissolved organic matter. Environ. Sci. Technol. 48, 10098–10106. https://doi.org/10.1021/es502670r.

Rahman, F., Rahman, M.M., Rahman, G.K.M.M., Saleque, M.A., Hossain, A.T.M.S., Miah, M.G., 2016. Effect of organic and inorganic fertilizers and rice straw on carbon sequestration and soil fertility under a rice–rice cropping pattern. Carbon Manag. 7, 41–53. https://doi.org/10.1080/17583004.2016.1166425.

Reba, M.L., Fong, B.N., Rijal, I., 2019. Fallow season CO2 and CH4 fluxes from US mid-south rice-waterfowl habitats. Agric. For. Meteorol. 279 https://doi.org/10.1016/j.agrformet.2019.107709.

Romero, C.M., Engel, R.E., D'Andrilli, J., Miller, P.R., Wallander, R., 2019. Compositional tracking of dissolved organic matter in semiarid wheat-based cropping systems using fluorescence EEMs-PARAFAC and absorbance spectroscopy. J. Arid Environ. 167, 34–42. https://doi.org/10.1016/j.jaridenv.2019.04.013.

Runkle, B.R.K., Seyfferth, A.L., Reid, M.C., Limmer, M.A., Moreno-García, B., Reavis, C. W., Peña, J., Reba, M.L., Adviento-Borbe, M.A.A., Pinson, S.R.M., Isbell, C., 2021. Socio-technical changes for sustainable rice production: rice husk amendment, conservation irrigation, and system changes. Front. Agron. 3, 1–14. https://doi.org/10.3389/fagro.2021.741557.

Runkle, B.R.K., Suvočarev, K., Reba, M.L., Reavis, C.W., Smith, S.F., Chiu, Y.L., Fong, B., 2019. Methane emission reductions from the alternate wetting and drying of rice fields detected using the eddy covariance method. Environ. Sci. Technol. 53, 671–681. https://doi.org/10.1021/acs.est.8b05535.

Seyfferth, A.L., Amaral, D., Limmer, M.A., Guilherme, L.R.G., 2019. Combined impacts of Si-rich rice residues and flooding extent on grain as and Cd in rice. Environ. Int. 128, 301–309. https://doi.org/10.1016/j.envint.2019.04.060.

Seyfferth, A.L., Fendorf, S., 2012. Silicate mineral impacts on the uptake and storage of arsenic and plant nutrients in rice (Oryza sativa L.). Environ. Sci. Technol. 46, 13176–13183. https://doi.org/10.1021/es3025337.

Seyfferth, A.L., Kocar, B.D., Lee, J.A., Fendorf, S., 2013. Seasonal dynamics of dissolved silicon in a rice cropping system after straw incorporation. Geochem. Cosmochim. Acta 123, 120–133. https://doi.org/10.1016/j.gca.2013.09.015.

Seyfferth, A.L., Morris, A.H., Gill, R., Kearns, K.A., Mann, J.N., Paukett, M., Leskanic, C., 2016. Soil incorporation of silica-rich rice husk decreases inorganic arsenic in rice grain. J. Agric. Food Chem. 64, 3760–3766. https://doi.org/10.1021/acs.jafc.6b01201.

Smith, P., Martion, D., Cai, Z., Gwary, D., Janzen, H., Kumar, P., McCarl, B., Ogle, S., O-Mara, F., Rice, C., Scholes, B., Sirotenko, O., 2007. Agriculture. In: Metz, B., Davidson, O.R., Bosch, P.R., Dave, R., Meyer, L.A. (Eds.), Climate Change 2007: Mitigation. Contribution of Working Group III to the Fourth Assessment Report of the Intergovernmental Panel on Climate Change. Cambridge University Press, Cambridge, United Kingdom, pp. 497–540. https://doi.org/10.1007/978-981-13-8429-5_5.

Stedmon, C.A., Bro, R., 2008. Characterizing dissolved organic matter fluorescence with parallel factor analysis: a tutorial. Limnol Oceanogr. Methods 6, 572–579. https://doi.org/10.4319/lom.2008.6.572.

Teasley, W.A., Limmer, M.A., Seyfferth, A.L., 2017. How rice (Oryza sativa L.) responds to elevated as under different Si-rich soil amendments. Environ. Sci. Technol. 51, 10335–10343. https://doi.org/10.1021/acs.est.7b01740.

Traina, S.J., Novak, J., Smeck, N.E., 1990. An ultraviolet absorbance method of estimating the percent aromatic carbon content of humic acids. J. Environ. Qual. 19, 151–153.

Verfaillie, J., Baldocchi, D., Variability, I., Ch, R., 2016. Biophysical controls on interannual variability in ecosystem-scale CO2 and CH4 exchange in a California rice paddy. J. Geophys. Res. Biogeosciences 978–1001. https://doi.org/10.1002/2015JG003247 (Received).

Verhoeven, E., Barthel, M., Yu, L., Celi, L., Said-pullicino, D., Sleutel, S., Lewicka-szczebak, D., Six, J., Decock, C., 2019. Early season N2O emissions under variable water management in rice systems: source-partitioning emissions using isotope ratios along a depth profile. Biogeosciences 16, 383–408. https://doi.org/10.5194/bg-16-383-2019.

Weishaar, J.L., Aiken, G.R., Bergamaschi, B.A., Fram, M.S., Fujii, R., Mopper, K., 2003. Evaluation of specific ultraviolet absorbance as an indicator of the chemical composition and reactivity of dissolved organic carbon. Environ. Sci. Technol. 37, 4702–4708. https://doi.org/10.1021/es030360x.

Wilson, H.F., Xenopoulos, M.A., 2009. Effects of agricultural land use on the composition of fluvial dissolved organic matter. Nat. Geosci. 2, 37–41. https://doi.org/10.1038/ngeo391.

Wu, X., Nguyen-Sy, T., Sun, Z., Wantanabe, T., Tawaraya, K., Hu, R., Cheng, W., 2020. Soil organic matter dynamics as affected by land use change from rice paddy to wetland. Wetlands 40, 2199–2207. https://doi.org/10.1007/s13157-020-01321-5.

Xionghui, J., Jiamei, W., Hua, P., Lihong, S., Zhenhua, Z., Zhaobing, L., Faxiang, T., Liangjie, H., Jian, Z., 2012. The effect of rice straw incorporation into paddy soil on carbon sequestration and emissions in the double cropping rice system. J. Sci. Food Agric. 92, 1038–1045. https://doi.org/10.1002/jsfa.5550.

Yamashita, Y., Nosaka, Y., Suzuki, K., Ogawa, H., Takahashi, K., Saito, H., 2013. Photobleaching as a factor controlling spectral characteristics of chromophoric dissolved organic matter in open ocean. Biogeosciences 10, 7207–7217. https://doi.org/10.5194/bg-10-7207-2013.

Ye, R., Horwath, W.R., 2017. Influence of rice straw on priming of soil C for dissolved organic C and CH 4 production. Plant Soil 417, 231–241. https://doi.org/10.1007/s11104-017-3254-5.

Yu, K., Patrick, W.H., 2003. Redox range with minimum nitrous oxide and methane production in a rice soil under different pH. Soil Sci. Soc. Am. J. 67, 1952–1958. https://doi.org/10.2136/sssaj2003.1952.

Zhang, W., Xu, M., Wang, X., Huang, Q., Nie, J., Li, Z., Li, S., Hwang, S.W., Lee, K.B., 2012. Effects of organic amendments on soil carbon sequestration in paddy fields of subtropical China. J. Soils Sediments 12, 457–470. https://doi.org/10.1007/s11368-011-0467-8.

Zhu, Z., Ge, T., Hu, Y., Zhou, P., Wang, T., Shibistova, O., Guggenberger, G., Su, Y., Wu, J., 2017. Fate of rice shoot and root residues, rhizodeposits, and microbial assimilated carbon in paddy soil - part 2: turnover and microbial utilization. Plant Soil 416, 243–257. https://doi.org/10.1007/s11104-017-3210-4.